

ASPECTS OF CONTACT METAMORPHISM  
PRODUCED BY THE NEW ENGLAND  
BATHOLITH, NEW SOUTH WALES

*by*

*Raymond Harry Roberts*

Thesis submitted for the degree  
of Doctor of Philosophy,  
University of New England,  
Armidale, N.S.W.

June, 1982.

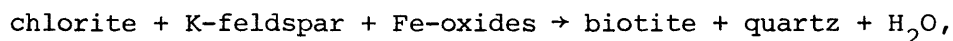
ABSTRACT

Forcefully emplaced plutons in the southern part of the New England Batholith, northern New South Wales, have produced extensive contact aureoles in Palaeozoic sediments and volcanics. This thesis describes the contact effects observed in pelitic, psammitic and impure calcareous sediments.

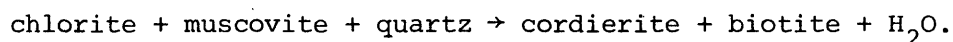
Four metamorphic zones are recognised within pelitic sediments around the Walcha Road Adamellite (with distances from the contact in brackets):

- I) biotite zone (4 km - 1500 m);
- II) cordierite zone (1500 m - 500 m);
- III) cordierite + K-feldspar zone (500 m - 100 m);
- IV) cordierite + K-feldspar ± garnet zone (100 m - contact).

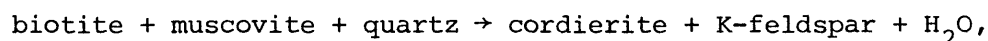
The two outer zone boundaries are defined by discontinuous reactions, the biotite isograd being represented by the general reaction



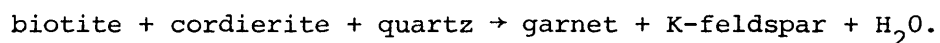
and the cordierite isograd by



Petrography and phase relations (probe data) demonstrate that, for any particular host-rock chemistry (specifically Mg/Mg+Fe ratio), these reactions can be represented as isothermal sections on divariant T-X(Fe-Mg) loops. The cordierite + K-feldspar isograd is defined by the continuous reaction



which shifts both biotite and cordierite Mg/Mg+Fe ratios toward more Fe-rich values along the divariant T-X(Fe-Mg) loop. The Mg/Mg+Fe ratios of phases participating in this reaction are fixed at the temperature at which muscovite is exhausted. They remain fixed unless a further temperature increase results in intersection of the divariant T-X(Fe-Mg) loop for the continuous reaction

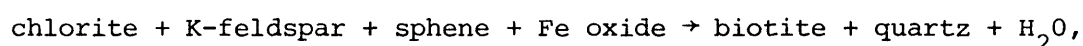


If intersected, this reaction causes a reversal in the Mg/Mg+Fe ratios of the ferromagnesian phases, shifting them to more Mg-rich values as temperature increases. All reactions in the pelites appear to take place on divariant reaction loops, and univariant reactions defined by the intersection of two or more divariant loops are not in evidence, apparently because reactants are consumed on the divariant curves before such intersections are achieved. At estimated pressures of 1-1½ kb, temperatures across the aureole are believed to range from 350-400°C at the outer limit to 720-745°C near the contact. Such contact temperatures are consistent with the observed presence at the contact of the Walcha Road Adamellite of migmatites believed to have formed by *in situ* partial melting of the pelites.

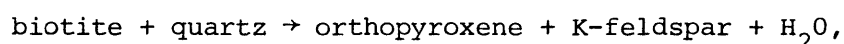
Mineralogical and textural changes define three metamorphic zones in greywackes around the Mt Duval Adamellite:

- I) blastopsammitic biotite zone (2½ km - 500 m);
- II) transitional biotite zone (500 m - 150 m);
- III) biotite + orthopyroxene zone (150 m - contact).

The biotite isograd is denoted by the discontinuous reaction



resulting in the loss of chlorite. The outer zone shows very little textural adjustment of the original sediment, and the onset of obvious textural modification defines the beginning of the transitional biotite zone. The orthopyroxene isograd is marked by the continuous reaction



which proceeds with an increase in the Mg/Mg+Fe ratio of both biotite and orthopyroxene. The high-grade zone is totally reconstituted, leaving little trace of original textures. Biotite compositions in the greywacke reflect the interrelated effects of paragenesis, host-composition, and structural and charge balance requirements, yielding a general decrease in Al, and increases in Ti and Mg with increasing grade. P-T conditions are not well delineated within the greywackes around the Mt Duval Adamellite. However, pressures of approximately 1 kb are suggested, and

temperatures appear to vary from 350<sup>o</sup>-400<sup>o</sup>C at the outer limit of the aureole to around 650<sup>o</sup>C at the contact.

The impure calcareous rocks comprise calcareous litharenites, impure calcirudites, impure biomicrites and stylolitic limestones with bulk rock compositions approximated by the  $K_2O$ -CaO-MgO- $Al_2O_3$ - $SiO_2$ - $CO_2$ - $H_2O$  system. Five metamorphic zones are delineated within these rocks around the Inlet Monzonite and Moonbi Adamellite:

- I) biotite zone (2 km - 1100 m);
- II) clinopyroxene zone (1100 m - 950 m);
- III) garnet zone (950 m - 650 m);
- IV) wollastonite zone (650 m - 350 m);
- V) wollastonite + plagioclase zone (350 m - contact).

These zones are based on mineralogical changes in the calcareous litharenites from the northern contact of the Inlet Monzonite (distances shown in brackets are for this aureole). They are also applicable to the impure calcirudites and biomicrites, except that no garnet zone occurs in the latter. The stylolitic limestones have a distinctive mineralogy (e.g. forsterite marble near the contact) that reflects a bulk-rock composition lower in  $SiO_2$ ,  $Al_2O_3$  and  $K_2O$  than that of the other calcareous rock types studied. Petrography and probe data reveal a prograde sequence of metamorphic reactions in the calcareous litharenites, which can be represented by a series of experimentally determined univariant curves on isobaric T- $X_{CO_2}$  diagrams for 1 and 2 kb corrected to allow for solid solution within the phases. Reactants and products of these reactions do not appear to coexist over significant temperature intervals, implying firstly that the reactions are discontinuous and secondly, that they do not buffer the pore-fluid composition. Contact metamorphic conditions in the calcareous litharenites of the northern aureole of the Inlet Monzonite are believed to have been approximately: pressure below 2 kb,  $X_{CO_2}$  in the fluid phase between 0.06 and 0.22, and temperatures ranging from around 350<sup>o</sup>C at the outer edge of the aureole ( $\approx$  2 km from the contact) up to 700-750<sup>o</sup>C at the contact.

Three types of small-scale reaction band are developed in calcirudites located 350m from the northern contact of the Inlet Monzonite; namely between (1) marble and pelite blocks, (2) garnet-rich matrix and

pelite blocks, and (3) garnet-rich matrix and marble blocks. They are believed to have formed during contact metamorphism at temperatures between 610 and 650°C and pressures below 2 kb. The characteristic sequence of layers developed between marble and pelite blocks is

marble  
 garnet  
 garnet + clinopyroxene  
 felsic (K-feldspar + sphene ± clinopyroxene ± plagioclase)  
 clinopyroxene + feldspar + sphene  
 biotite + feldspar + sphene  
 biotite + feldspar unit  
 pelite (unmodified material not found)

The original contact between marble and pelite is represented by the boundary between the garnet + clinopyroxene and felsic layers. This boundary is characterised texturally by a sharp change in grain size, and mineralogically by the lack of K<sub>2</sub>O- and TiO<sub>2</sub>-bearing phases on the marble side. The layer sequence developed between the garnet-rich matrix and pelite blocks is similar to that in the marble → pelite reaction bands. At contacts between matrix and marble blocks, either a monominerallic wollastonite layer, or a wollastonite + garnet + clinopyroxene layer is developed within the original marble. Chemical variations across the reaction bands, calculated from modal data and microprobe analyses, show sharp changes in composition at layer boundaries. Notably, CaO shows a stepwise decrease across the reaction band away from the marble, whereas Al<sub>2</sub>O<sub>3</sub> and MgO (+FeO) decrease away from the pelite, but increase in the garnet and garnet + clinopyroxene layers respectively.

The reaction bands are believed to have developed by mass transfer of components between chemically incompatible adjacent rock types. A model is suggested whereby the components diffuse through a pore solution in response to chemical potential gradients in the solution (concentration gradients). These gradients are maintained by removal of material from solution, as solid phases in equilibrium with the fluid are formed in the reaction bands. Diffusion proceeds so as to reduce these gradients and, with time, discontinuities are eliminated and the chemical potentials of the diffusing components will vary monotonically and continuously across the reaction band. Local equilibrium is considered to be achieved at each point across the reaction band. The solid phases in local equilibrium with the diffusing components of the pore fluid can be expressed on chemical

potential diagrams. The layers develop across the reaction band as new phases become stable in response to the continuously changing chemical potentials of the diffusing components and the presence or absence of non-diffusing components. The layers represent distinct changes in mineral assemblage, and the layer boundaries mark sharp discontinuities in bulk-rock composition. The number of phases in each layer is typically less than the number of components. The relationship between the number of phases and components can be expressed by the phase rule in terms of J- and K- components (Thompson, 1970). Flux (amount of material moved) appears to be directly related to differences in the concentrations of components between the two initially chemically incompatible rock types. The relative distances to which the components have diffused across the original boundary appear to depend simply on the flux of each component and the rate at which it is used by the solid phases forming in equilibrium with the pore fluid.

#### ACKNOWLEDGEMENTS - Addendum

Two earlier oversights need correcting. Firstly, I acknowledge Graham Teale for his help in the initial choosing of my thesis topic, and for allowing me to see his B.A. Honours thesis (Teale, 1974) which was carried out in the New England region. Secondly I thank Basil Flinter for many interesting discussions, not all of which were geologically based.

## ACKNOWLEDGEMENTS

I am sincerely grateful to Dr. N.C.N. Stephenson for his meticulous supervision which greatly improved this thesis. I thank him for his patience and understanding, and for all those hours so freely given. The remainder of the academic and technical staff of the Geology Department at the University of New England are thanked for their assistance. Nick Ware of the Research School of Earth Sciences, Australian National University, is acknowledged for making available the electron microprobe and for his kindness during my stay in Canberra.

To my fellow post-graduate students, in particular Ken Cross, Chris Fergusson, Bob Haydon, Jocelyn McPhie, Joe Stolz and Colin Turner, I express my deepest gratitude for their help and encouragement. I also thank them for their friendship both at work and socially, and most of all for understanding the traumas associated with doing a Ph.D. Thanks also to Kerin Cross, Barbara Haydon and Kerrie Stolz for their kindness, and wonderful cooking. Fellow residents of Perrott Street, Jeffery Street, Mann Street and Mary White are thanked for many good memories. Paul (Spook) Spry is also acknowledged for his postcards.

Tony Gates is thanked for his excellent drafting of a seemingly never-ending number of figures. To Rita Cuskelly, who typed the early drafts and the final copy of this thesis, my greatest appreciation for a terrific effort.

Special thanks are given to Mum, Dad and the rest of my family for their continued support and love. To Christine mere thanks are not enough; for all your help, encouragement, tolerance and thoughtfulness I love you.



TABLE OF CONTENTS

	Page No.
ABSTRACT	i
ACKNOWLEDGEMENTS	vi
TABLE OF CONTENTS	vii
LIST OF FIGURES	xiv
LIST OF TABLES	xvii
LIST OF PLATES	xix
<u>CHAPTER ONE</u>	
<u>INTRODUCTION</u>	
1.1 <u>PREAMBLE</u>	1
1.2 <u>AIMS AND APPROACH</u>	1
1.3 <u>GEOLOGICAL SETTING</u>	5
1.3.1 Introduction	5
1.3.2 The Palaeozoic Sediment and Volcanics	6
1.3.3 The New England Batholith	8
1.3.4 Regional Tectonic Development	11
1.4 <u>CONTACT AUREOLES AND ROCK TYPES INVESTIGATED</u>	12
1.4.1 Plutons	12
1.4.2 Rock Types	13
Pelitic Rocks	13
Psammitic Rocks	13
Impure Calcareous Rocks	13
Basic Volcanics	15
1.5 <u>PREVIOUS INVESTIGATIONS</u>	15
1.6 <u>GENERAL CHARACTERISTICS OF THE IGNEOUS CONTACTS AND METAMORPHIC AUREOLES</u>	16
1.6.1 Pluton-to-Aureole Contacts	16
1.6.2 Aureole Widths	17
1.6.3 General Structural Trends	19
1.6.4 Mode of Pluton Emplacement	19

CHAPTER TWOPELITIC ROCKS

	Page No.
2.1 <u>INTRODUCTION</u>	24
2.2 <u>GEOCHEMISTRY</u>	24
2.3 <u>PETROGRAPHY OUTSIDE THE AUREOLE</u>	30
2.4 <u>PETROGRAPHY OF THE CONTACT METAMORPHOSED ROCKS</u>	30
2.4.1 Introduction	30
2.4.2 Biotite Zone	32
2.4.3 Cordierite Zone	32
2.4.4 Cordierite + K-feldspar Zone	36
2.4.5 Cordierite + K-feldspar ± Garnet Zone	38
2.4.6 Migmatite Outcrops	41
2.5 <u>MINERAL CHEMISTRY</u>	42
2.5.1 Introduction	42
2.5.2 Feldspar	42
2.5.3 Chlorite	42
2.5.4 Muscovite	43
2.5.5 Biotite	43
2.5.6 Cordierite	48
2.5.7 Garnets	48
2.5.8 Opaques	48
2.6 <u>METAMORPHIC REACTIONS</u>	52
2.6.1 Introduction	52
2.6.2 Biotite Isograd	52
2.6.3 Cordierite Isograd	56
2.6.4 Cordierite + K-feldspar Isograd	57
2.6.5 Garnet Isograd	58
2.6.6 Retrograde Reactions	60
2.7 <u>PHASE RELATIONS</u>	61
2.7.1 Introduction	61
2.7.2 Discontinuous and Continuous Reactions	61
2.7.3 Phase Relations in the Walcha Road Aureole	63
Biotite Isograd	63
Cordierite Isograd	67
Cordierite + K-feldspar Isograd	68
Garnet Isograd	69
2.7.4 Distribution Coefficients	71
2.7.5 Summary of Conclusions	73
2.8 <u>MIGMATITITE PETROGENESIS</u>	73

2.9	<u>P-T CONDITIONS</u>	79
	2.9.1 Biotite Isograd	82
	2.9.2 Cordierite Isograd	82
	2.9.3 Cordierite + K-feldspar Isograd	83
	2.9.4 Contact Temperatures	83
2.10	<u>SUMMARY</u>	83

### CHAPTER THREE

#### PSAMMITIC ROCKS (GREYWACKES)

3.1	<u>INTRODUCTION</u>	87
3.2	<u>GEOCHEMISTRY</u>	87
3.3	<u>PETROGRAPHY OUTSIDE THE AUREOLE</u>	91
3.4	<u>PETROGRAPHY OF THE CONTACT METAMORPHOSED ROCKS</u>	95
	3.4.1 Blastopsammitic Biotite Zone	95
	3.4.2 Transitional Biotite Zone	97
	3.4.3 Biotite + Orthopyroxene Zone	100
3.5	<u>MINERAL CHEMISTRY</u>	101
	3.5.1 Introduction	101
	3.5.2 Feldspar	102
	3.5.3 Biotite	102
	3.5.4 Orthopyroxene	110
	3.5.5 Ilmenite	110
	3.5.6 Retrograde Chlorite	110
	3.5.7 Retrograde Amphiboles	110
3.6	<u>METAMORPHIC REACTIONS AND PHASE RELATIONS</u>	113
	3.6.1 Reactions of Regional Metamorphism	113
	3.6.2 Reactions and Phase Relations of Contact Metamorphism	114
	Biotite Isograd	114
	Transitional Biotite Zone	118
	Orthopyroxene Isograd	119
3.7	<u>DISCUSSION OF BIOTITE CHEMISTRY AND ROCK TYPE</u>	121
3.8	<u>P-T CONDITIONS</u>	122
3.9	<u>SUMMARY</u>	124

CHAPTER FOURIMPURE CALCAREOUS ROCKS

	Page No.
4.1 <u>INTRODUCTION</u>	127
4.2 <u>PETROGRAPHY AND METAMORPHISM OUTSIDE THE AUREOLES</u>	129
4.3 <u>LOCALITIES AND ROCK TYPES INVESTIGATED</u>	129
4.3.1 Horse Arm Creek	131
4.3.2 South Kootingal	133
4.3.3 Seven Mile Creek	133
4.4 <u>PETROGRAPHY OF THE CONTACT METAMORPHOSED ROCKS</u>	133
4.4.1 Introduction	133
4.4.2 Calcareous Litharenites	136
Outside the Aureole	136
Biotite Zone	136
Clinopyroxene Zone	136
Garnet Zone	138
Wollastonite Zone	140
Wollastonite + Plagioclase Zone	140
4.4.3 Impure Calcirudites	141
Outside the Aureole	141
Horse Arm Creek	142
South Kootingal	142
Seven Mile Creek	143
4.4.4 Impure Biomicrites	143
4.4.5 Stylolitic Limestones	144
4.5 <u>MINERAL CHEMISTRY</u>	145
4.5.1 Introduction	145
4.5.2 Low-Grade Ferromagnesians-Chlorite, Biotite, Amphibole, Clinopyroxene	145
4.5.3 Garnet	147
4.5.4 Clinopyroxene (with garnet)	147
4.5.5 Epidote	150
4.5.6 Plagioclase	150
4.6 <u>METAMORPHIC REACTIONS AND PHASE RELATIONS</u>	150
4.6.1 Introduction	150
4.6.2 Calcareous Litharenites	152
Outside the Aureole	152
Biotite Isograd	152
Clinopyroxene Isograd	155
Garnet Isograd	160
Wollastonite Isograd	161
Wollastonite + Plagioclase Isograd	162
4.6.3 Impure Biomicrites	163
4.6.4 Discussion of the Mineralogy and Bulk-Rock Composition of the Stylolitic Limestones	164

4.7	<u>METAMORPHIC CONDITIONS</u>	165
4.7.1	Discussion of T-X <sub>CO<sub>2</sub></sub> Diagrams	165
4.7.2	Calcareous Litharenites	168
	Buffering of the Pore Fluid	168
	XCO <sub>2</sub> in the Fluid Phase	172
	Biotite Zone	172
	Clinopyroxene Zone	173
	Garnet Zone	174
	Wollastonite-bearing Zones	176
	Conclusions	177
4.7.3	Impure Calcirudites	177
4.7.4	Impure Biomicrites	177
4.8	<u>SUMMARY</u>	178

## CHAPTER FIVE

### CALC-SILICATE REACTION BANDS

5.1	<u>INTRODUCTION</u>	181
5.2	<u>LOCATION AND FIELD DESCRIPTION</u>	181
5.3	<u>P-T CONDITIONS</u>	185
5.4	<u>PETROGRAPHY</u>	185
5.4.1	Introduction	185
5.4.2	Mable → Pelite Reaction Bands	187
	Marble	189
	Garnet Layer	189
	Garnet + Clinopyroxene Layer	189
	Felsic Layer	189
	Clinopyroxene + Feldspar + Sphene Layer	191
	Biotite + Feldspar + Sphene Layer	191
	Biotite + Feldspar Unit	191
	Sulphides Within the Layers	192
	Clinopyroxene + Garnet : Felsic Layer Boundary	192
5.4.3	Garnet-rich Matrix → Pelite Reaction Bands	193
	Garnet-rich Matrix	193
	Garnet-Clinopyroxene Layer	193
	Garnet+Clinopyroxene Layer → Biotite+Feldspar Unit	194
5.4.4	Garnet-rich Matrix → Marble Reaction Bands	195
5.5	<u>MINERAL CHEMISTRY</u>	195
5.5.1	Introduction	195
5.5.2	Garnet	195
5.5.3	Clinopyroxene	203
5.5.4	Biotite	204
5.5.5	Feldspar	204
5.5.6	Other Phases	205

5.6	<u>CHEMICAL VARIATION ACROSS THE REACTION BANDS</u>	205
	5.6.1 Layer Compositions	205
	5.6.2 Chemical Trends	208
	5.6.3 ACF Diagrams	213
5.7	<u>MASS BALANCE CALCULATIONS</u>	215
	5.7.1 Introduction	215
	5.7.2 Results and Discussion	216
	5.7.3 Summary and Conclusions	219
5.8	<u>REACTIONS</u>	220
	5.8.1 Biotite + Feldspar Unit	220
	5.8.2 Biotite + Feldspar + Sphene Layer	221
	5.8.3 Clinopyroxene + Feldspar + Sphene Layer	223
	5.8.4 Further Discussion	223
5.9	<u>PETROGENESIS OF THE REACTION BANDS</u>	223
	5.9.1 Introduction and Review	223
	5.9.2 Formation of the Marble → Pelite Reaction Bands	226
	Garnet Layer	230
	Garnet + Clinopyroxene Layer	230
	Layers on the Pelite Side of the Original Boundary	231
	Summary and Discussion	233
	5.9.3 Relative Movement of the Components	236
	Flux	236
	Distances Moved	237
	5.9.4 Volatile Distribution	238
	5.9.5 Felsic Layer	239
	5.9.6 Reaction Bands Involving the Garnet-rich Matrix	239
	Garnet-rich Matrix	239
	Garnet-rich Matrix → Pelite Reaction Bands	240
	Garnet-rich Matrix → Marble Reaction Bands	240
	Discussion	241
5.10	<u>FURTHER EXAMPLES OF REACTION BANDS</u>	241
	5.10.1 Sample T77B	241
	5.10.2 Sample T73A	242
	5.10.3 Discussion	242
5.11	<u>LARGER-SCALE DIFFUSION</u>	243
5.12	<u>SUMMARY AND CONCLUSIONS</u>	247

CHAPTER SIXSUMMARY OF CONCLUSIONS AND SYNTHESIS

6.1	<u>PELITIC ROCKS</u>	252
6.2	<u>PSAMMITIC ROCKS</u>	254
6.3	<u>IMPURE CALCAREOUS ROCKS</u>	256
6.4	<u>CALC-SILICATE REACTION BANDS</u>	258
6.5	<u>SYNTHESIS</u>	261
6.6	<u>SUGGESTIONS FOR FURTHER WORK</u>	265
	<u>REFERENCES</u>	266
	APPENDIX I - Geological map of the skarn locality shown in Figure 4-2	278
	APPENDIX II - Chemical analyses of basalts from the Mt Duval aureole	279
	APPENDIX III	281
	APPENDIX IV - Analytical Methods	283
	APPENDIX V - Rock Catalogue	285

LIST OF FIGURES

<u>Figure No.</u>	<u>Title</u>	<u>Page No.</u>
1-1	Location of the New England Fold Belt and study area	2
1-2	Distribution of stratigraphic associations and Palaeozoic igneous rocks as defined by Korsch (1977)	7
1-3	The distribution of the plutonic suites and leucoadamellites in the New England Batholith, as defined by Shaw and Flood (1981)	9
1-4	General geology of the study area	14
1-5	The general structural trend within the southern part of the New England Fold Belt in the vicinity of Armidale and Tamworth	20
2-1	The location of areas studied around the Walcha Road Adamellite	25
2-1A	Sample location map for the southeast contact aureole of the Walcha Road Adamellite	26
2-1B	Sample locality map for the southwest contact aureole of the Walcha Road Adamellite	27
2-1C	Sample locality map for the western contact aureole of the Walcha Road Adamellite	28
2-2	Schematic representation of the variation in modal composition of pelitic hornfeldes with increasing grade in the aureole of the Walcha Road Adamellite	31
2-3	Biotite chemistry versus distance from the contact of the Walcha Road Adamellite	45
2-4	Cordierite Mg/Mg+Fe ratio ( $X_{Mg}^{Cd}$ ) versus distance from the contact of the Walcha Road Adamellite	49
2-5	AKF diagrams for the Walcha Road Adamellite contact aureole	53
2-6	AFM diagrams for the Walcha Road Adamellite contact aureole	54
2-7	Schematic T-X(Fe-Mg) diagram for low-pressure contact metamorphism of pelites	64



<u>Figure No.</u>	<u>Title</u>	<u>Page No.</u>
2-8	Mg-Fe distribution coefficient for biotite and cordierite ( $K_{D(Mg)}^{Bi-Cd}$ ) versus the Mg/Mg+Fe ratio of biotite ( $X_{Mg}^{Bi}$ )	72
2-9	Cotectic lines at 1 and 2 kb $P_{H_2O}$ for the Qz-Ab-Or-An tetrahedron projected from the An apex onto the Qz-Ab-Or face	78
2-10	P-T diagram showing univariant reactions relevant to the contact metamorphism of pelites	80
3-1	Sample locality map of greywackes from the Mt Duval Adamellite and Uralla Granodiorite contact aureoles	88
3-2	Variations in major-element chemistry with distance from the contact	90
3-3	Variations in trace-element chemistry from the contact	92
3-4	Biotite mineral chemistry versus distance from the contact of Mt Duval Adamellite	103
3-5	Correlations between the elements substituting in the biotite octahedral layer	106
3-6	Schematic T-X(Fe-Mg) diagram for the greywackes in the Mt Duval Adamellite and Uralla Granodiorite contact aureoles	116
3-7	Variation in the biotite Al/Al+Ti ratio with increasing grade of contact metamorphism, for greywackes in the Mt Duval Adamellite and Uralla Granodiorite contact aureoles	117
4-1	The location of areas at which contact metamorphism of the impure calcareous rocks has been studied	128
4-2	Geological and sample locality map for the Horse Arm Creek locality	132
4-3	Geological and sample locality map for the South Kootingal locality	134
4-4	Geological and sample locality map for the Seven Mile Creek locality	135
4-5	ACF diagrams for the calcareous litharenites at the Horse Arm Creek locality	153
4-6	Schematic T-X(Fe-Mg) diagram for the reaction $Bi+Cal+Qtz \rightarrow Cpx+K-f+H_2O+CO_2$	157

<u>Figure No.</u>	<u>Title</u>	<u>Page No.</u>
4-7	T-X <sub>CO<sub>2</sub></sub> diagram at 1 kb for some equilibria in the system K <sub>2</sub> O-CaO(Na <sub>2</sub> O)-MgO(FeO)-Al <sub>2</sub> O <sub>3</sub> (Fe <sub>2</sub> O <sub>3</sub> )-SiO <sub>2</sub> -CO <sub>2</sub> -H <sub>2</sub> O	169
4-8	T-X <sub>CO<sub>2</sub></sub> diagram at 2 kb for some equilibria in the system K <sub>2</sub> O-CaO(Na <sub>2</sub> O)-MgO(FeO)-Al <sub>2</sub> O <sub>3</sub> (Fe <sub>2</sub> O <sub>3</sub> )-SiO <sub>2</sub> -CO <sub>2</sub> -H <sub>2</sub> O	170
4-9	Schematic representation of the intersection of curves 9 and 10 (Fig. 4-7), as a result of Fe substitution in the phases	175
5-1	Location of the costean (sample locality 371) from which the major examples of calc-silicate reaction bands were sampled	183
5-2	Profiles of mineral composition across selected reaction bands	196
5-3	Concentration of oxide components (moles per 100 cm <sup>3</sup> ) across selected reaction bands	209
5-4	ACF diagrams of bulk composition across the reaction bands	214
5-5	Schematic chemical potential diagram for SiO <sub>2</sub> -CaO-AlO <sub>3/2</sub> (plus the μSiO <sub>2</sub> -μCaO projection, Fig. 5.5A)	228
5-6	Schematically superimposed chemical potential diagrams for the systems SiO <sub>2</sub> -CaO-AlO <sub>3/2</sub> and SiO <sub>2</sub> -CaO-MgO (plus the μSiO <sub>2</sub> -μCaO projection, Fig. 5.6A)	232
5-7	Schematically superimposed μSiO <sub>2</sub> -μCaO projections for the systems SiO <sub>2</sub> -CaO-AlO <sub>3/2</sub> and SiO <sub>2</sub> -CaO-MgO	234
5-8	Schematic representation of the chemical potentials of the components in the pore fluid across the marble → pelite reaction bands	235
6-1	Diagrammatic representation of metamorphic zones in specific contact aureoles in the southern part of the New England Batholith assuming pressures between 1 and 1½ kb	262

LIST OF TABLES

<u>Table No.</u>	<u>Title</u>	<u>Page No.</u>
1.1	Relative widths of the contact aureoles around selected plutons in the southern part of the New England Batholith	18
2.1	Chemical analyses of contact-metamorphosed pelitic and semi-pelitic sediments	29
2.2	Representative microprobe analyses of minerals from lower-grade zones in the Walcha Road aureole	44
2.3	Representative microprobe analyses of minerals from higher-grade zones in the Walcha Road aureole	47
2.4	Microprobe analyses showing the effects of progressive cordierite alteration	50
2.5	Microprobe ilmenite analyses from pelites of varying grade in the Walcha Road aureole	51
2.6	Biotite and plagioclase analyses from the migmatized sample 391 and the Walcha Road Adamellite	75
2.7	Modal analyses of the leucocratic material plotted in Fig. 2-9	77
3.1	Chemical analyses of greywackes from the Mt Duval aureole	89
3.2	Representative microprobe analyses of minerals in greywackes outside the Mt Duval aureole	94
3.3	Modes of greywackes from the Mt Duval aureole showing variation with increasing grade of contact metamorphism	96
3.4	Variations in biotite chemistry with increasing grade in the Mt Duval Adamellite and Uralla Granodiorite aureoles	108
4.1	Microprobe analyses of prehnite, pumpellyite and chlorite from sample T68 (outside the aureole)	130
4.2	Microprobe analyses of low-grade biotite, chlrite, amphibole and clinopyroxene in impure calcareous rocks	146
4.3	Microprobe analyses of garnets in impure calcareous rocks	148
4.4	Microprobe analyses of clinopyroxenes (with garnet) in impure calcareous rocks	149

<u>Table No.</u>	<u>Title</u>	<u>Page No.</u>
4.5	Microprobe analyses of epidotes in impure calcareous rocks	151
5.1	Modal analyses of selected traverses across reaction bands from sample locality 371	188
5.2A	Typical microprobe analyses from traverse 371-1A	198
5.2B	Typical microprobe analyses from traverse 371-VS2	199
5.2C	Typical microprobe analyses from traverse 371-1B	200
5.2D	Typical microprobe analyses from traverse 371-VI	201
5.2E	Typical microprobe analyses from traverse 371-L	202
5.3	Molar volumes ( $\text{cm}^3$ ) used in calculating Table 5.4	206
5.4	Moles of oxide constituents per $100 \text{ cm}^3$ within the layers of the calc-silicate reaction bands	207
5.5	Mass-balance calculations of oxide components across the marble $\rightarrow$ pelite reaction band traverse 371-1A (based on constant volume)	217
5.6	Conversion of modal per cent to moles per $100 \text{ cm}^3$ for part of traverse 371-1A	222
5.7	Representative microprobe analyses from samples T82A and T82C	245
5.8	Comparative chemical analyses of samples T82C and T82A	246

LIST OF PLATES

<u>Plate No.</u>	<u>Title</u>	<u>Page No.</u>
2-1	Textures in pelites from the outer zones of the Walcha Road Adamellite aureole	33
2-2	Textures in pelites from the inner zones of the Walcha Road Adamellite aureole	37
3-1	Textural variation in the greywackes with increasing grade of contact metamorphism. Photographs taken under crossed polars	98
3-2	Textural variation in the greywackes with increasing grade of contact metamorphism. Photographs taken under plane-polarised light	99
4-1	Textures in calcareous litharenites from the Horse Arm Creek locality (at grades below the clinopyroxene isograd)	137
4-2	Textures in calcareous litharenites from the Horse Arm Creek locality (at grades above the clinopyroxene isograd)	139
5-1	Hand specimen photographs of reaction bands within impure calcirudite from the costean at sample locality 371 in the northern aureole of the Inlet Monzonite	184
5-2	Hand specimen photographs of reaction bands in sample 371-1 from the northern aureole of the Inlet Monzonite	186
5-3	Photomicrographs of the layer sequence across the marble → pelite reaction band in sample 371-1 (i.e. traverse 371-1A)	190